ORIGINAL PAPER

Oil removal from water using highly hydrophobic, ultralight carbon microspheres

P. Bakhshi[1] · H. Tavakol[1]

Abstract
In the present work, the chemical vapor deposition method was employed for the preparation of highly hydrophobic and ultralight carbon spheres from cheap and available starting material and catalyst, acetylene and bentonite. This methodology was highly repeatable and could be easily scaled up for industrial purposes. In this line, the effect of the growth's temperature on the morphology of the product was investigated. The highly uniform products were obtained at different temperatures (650–800 °C), but the most uniform spheres were obtained at 750 °C. Tunneling electron microscope images proposed the hollowed shapes for prepared spheres, and its calculated density (5.08 mg/cm^3) confirmed this suggestion and proposed that this material could be considered as ultralight material or aerogel. The morphology and chemical structure of the product was also examined using field emission scanning electron microscopy, Raman and X-ray diffraction analyses. The thermogravimetric analysis showed a high thermal resistance of the product and less than 4% weight loss was observed up to 620 °C. The high hydrophobic nature of the product (with static contact angle = 130°) makes it as a potential candidate for oil absorption from the water, and its fast and high oil adsorption potencies were confirmed via the common experiment.

Graphic abstract

Highly hydrophobic carbon microspheres powder

TEM image
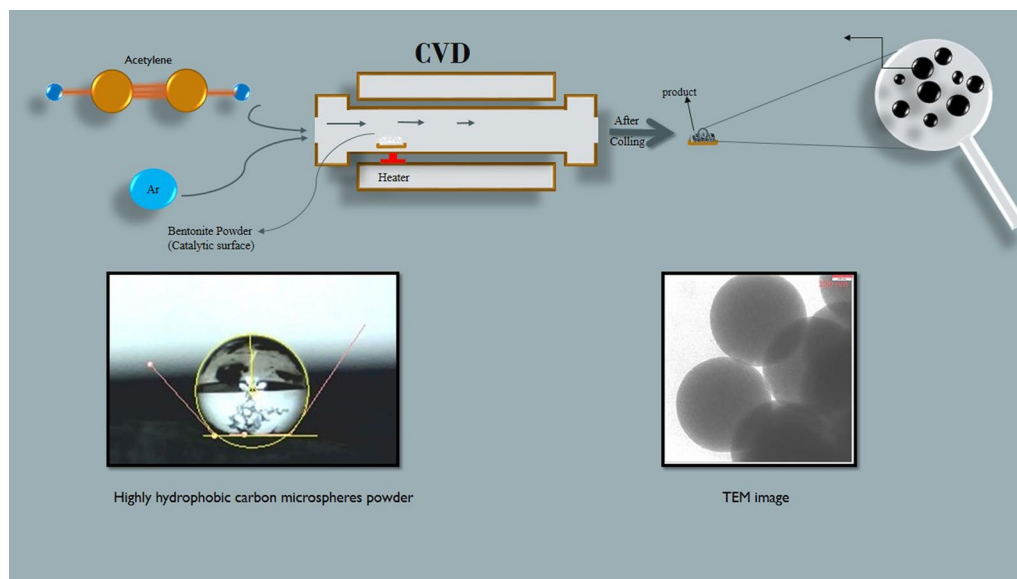
Editorial responsibility: Binbin Huang.

Extended author information available on the last page of the article

Introduction

Carbon porous materials (or activated carbon materials, ACMs) have been considered since a long time ago for scientific and industrial purposes (Deshmukh et al. 2010; Evans et al. 1999; Frolich 1936; Lee et al. 2006; Liang et al. 2008; Slyh et al. 1950). The carbon element has different allotropes and shapes, such as fullerenes, nanotubes and diamond (Falcao and Wudl 2007; Hoffmann et al. 2016). The ACMs have been employed in several applications by the scientists in different fields (Shafeeyan et al. 2010; Zheng and Xia 2017; Sung et al. 2018; Yang et al. 2011). During recent years, demand for such products has been increasing and is expected to continue to increase in the future. The global market for activated carbon is expected to be increased to 9.5% in 2022. Because of the increase in using these materials, they should be produced in higher quantities. In this line, developing new and more efficient methodologies that use the simpler and faster method and cheaper starting materials, catalysts and instruments is necessary to produce these materials and answer to their high demands.

For the production of carbon-based materials, different methods such as decomposing organic structures, chemical vapor deposition (CVD), arc discharge have been developed (Kumar and Ando 2010). Among various methods, the CVD method is the most appropriate method, especially for the large-scale preparations, because of its simplicity and ability to use various cheap and available starting materials (Manawi et al. 2018). Using the CVD method, various types of carbon materials such as graphenes, nanotubes and carbon spheres could be prepared. Spherical or ball structures are one of the forms of carbon allotropes with high porosity that can have the graphitic network or not (Deshmukh et al. 2010). Carbon spheres (CSs) have different uses in the fields of hydrogen storage (Jiang et al. 2010), fuel cells (Wen et al. 2007), composites material (Wu et al. 2015; Sichel et al. 1978), batteries (Liang et al. 2011; Jun et al. 2014), capacitors (Li et al. 2007, 2011), adsorbents (Dubey et al. 2014; Lu et al. 2006; Wickramaratne and Jaroniec 2013) and catalyst supports (Wu et al. 2008; Han et al. 2017). By reviewing the literature, there is a report in 2004, using CVD for preparation of CSs from acetylene and transition metal salts supported on kaolin at a temperature range 750–850 °C (Miao et al. 2004). Another report in the same year was published by Peng et al. for the preparation of CSs using CVD from toluene without a catalyst at the temperature above 1000 °C (Qian et al. 2004). Jin et al. produced CSs from the pyrolysis of hydrocarbons on a quartz substrate at temperatures between 900 and 1200 °C using the CVD method (Jin et al. 2005). However, despite the high importance and vast applications of CSs the existed methods for their preparation have some limitations, which make developing their new

preparation methods interesting for scientists. Therefore, in the course of previous studies on the synthesis and applications of carbon nanostructures (Tavakol and Keshavarzipour 2016; Mohammadi and Tavakol 2018; Hassani and Tavakol 2018; Manoukian et al. 2018), it was focused on the synthesis of CSs with special properties using CVD method. The main goal of this project is using cheap and available starting materials and catalyst, inexpensive production (by considering the costs of the instrument and consuming energy) and the scale-up ability of the procedure for industrial purpose. In the reported studies, they used high temperature or expensive catalysts and these issues should be solved. Moreover, the product was employed for the adsorption of oil from water and its wettability was examined. The details of experiments and related discussions will be presented in the next sections. All parts of this project have been done in the Nanocarbon Laboratory, Department of Chemistry, Isfahan University of Technology, during 2017–2018.

Materials and methods

Bentonite was purchased from Sepeed Powder Company (Kashan, Iran) and gas sources bought from Tebgas Co. (Isfahan, Iran). Oleic acid and other chemicals and solvents were obtained from Merck Co. The growth of the CS was carried out via a handmade double-zone electric tube furnace (Nanosat Co, Semnan, Iran; www.nanosatco.com). FESEM and EDS experiments were performed using Mira 3-XMU FESEM (Tescan Co, Brno, Czech Republic). Raman spectra were recorded by Senterra instrument (Bruker Co, USA), and XRD analyses were obtained from X'pert instrument (Philips Co, the Netherlands). DTA and TGA experiments were performed in an inert atmosphere, using Thermoanalyser STA 503 (BAHR, Germany) with 10 °C/min heating rate in the presence of alumina as a reference and 5 mg of sample. TEM images were recorded using EM208S TEM microscope from Philips Co (the Netherlands).

The preparation and purification of the product

The preparation of the catalytic substrate was simple. First, the bentonite powder was placed on the alumina boat without any pretreatment and modification. To study the growth temperature of the products, several temperatures including 650, 750 and 800 °C were considered for the growth step, which 750 °C showed the best results and chosen as the optimum temperature. After setting the temperature on 750 °C (under argon atmosphere), acetylene gas flowed at 200 ml/min for 20 min. Then, the heating was stopped and let the CVD to be cooled. The product was gathered from the alumina boat and easily removed from the catalyst without any workup or chemical process.

The oil adsorption experiments

For these experiments, different values of oleic acid (10 20, 30, …, 250 mg) were used to examine the extreme adsorption capacity of the adsorbent. In each experiment, the oleic acid was added to the water with vigorous mechanical stirring. After the observation of the uniform emulsion, 10 mg of adsorbent (m_{CS}) was added to the mixture and it was stirred for a couple of seconds. Then, the solution was filtrated, the oily–solid (oil-adsorbent) mixture was washed three timed with distilled water and dried in the oven at 100 °C for 1 h and then, it was weighted to obtain the total weight of the adsorbent plus adsorbed oil. The value of experimental adsorption capacity (q_m) of the product was obtained by weighting using Eq. 1:

$$q_m = m_{oil}/m_{CS} \tag{1}$$

where m_{CS} is the weight of CS before oil absorption (in g), m_{oil} is the maximum weight of adsorbed oil (in mg) and q_m is the experimental adsorption capacity (mg/g).

The adsorption (removal) efficiency (q_e, in percent) was obtained using Eq. 2, in which m_t ($m_t \leq m_{oil}$) is the total weight of added oil (in mg) and m_f is the final weight of the CS + oil.
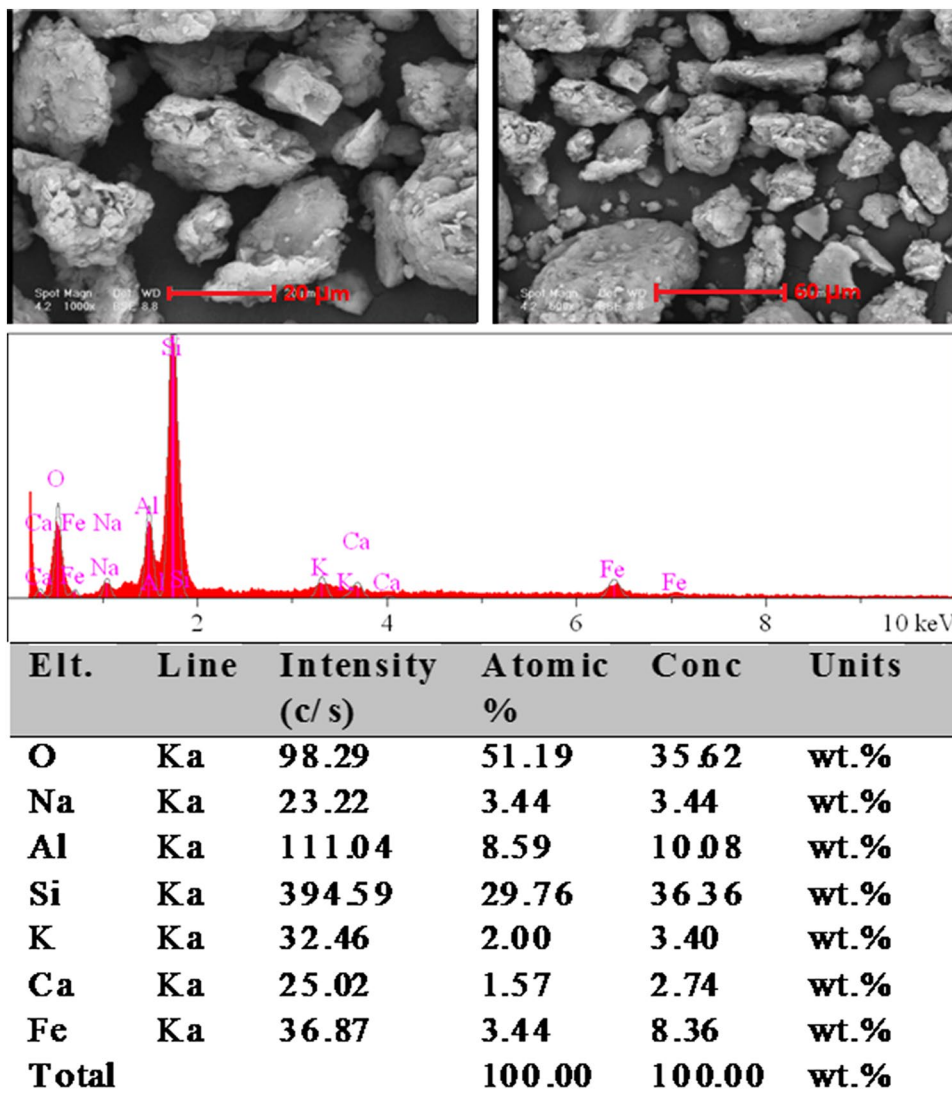
$$q_e (\%) = (m_f - m_{CS}) \times 100/m_t \tag{2}$$

For the investigation of the adsorption kinetics, because of the ultrafast adsorption process, the whole of this process was completed in less than one second and it was not possible to study the kinetic models.

Results and discussion

As described in the previous section, any preparation or pretreatment for the employed catalyst (bentonite) was not needed. However, first its structure and chemical composition were analyzed using SEM–EDX analyses and the results are shown in Fig. 1. According to this figure, the

Fig. 1 SEM–EDX analyses of bentonite as employed catalyst

Elt.	Line	Intensity (c/s)	Atomic %	Conc	Units
O	Ka	98.29	51.19	35.62	wt.%
Na	Ka	23.22	3.44	3.44	wt.%
Al	Ka	111.04	8.59	10.08	wt.%
Si	Ka	394.59	29.76	36.36	wt.%
K	Ka	32.46	2.00	3.40	wt.%
Ca	Ka	25.02	1.57	2.74	wt.%
Fe	Ka	36.87	3.44	8.36	wt.%
Total			100.00	100.00	wt.%

sizes of bentonite particles are between 5 and 50 μm. It is consisted of Al, Na, Fe, K and Ca elements, in addition to its silica structures. These metal elements play an important role in the production of carbon materials. As normally did for every CVD experiment, various experimental parameters such as the rates of carrier gases, the growth time, the place and nature of support (alumina or quartz boat) were optimized in several primary experiments. After the optimization of basic growth parameters, since it was proved that the growth's temperature is an effective parameter on the morphology and size of the product (Mohammadi and Tavakol 2018; Hassani and Tavakol 2018), different growth temperatures were employed. The FESEM images of the products at 650 (CS650), 750 (CS750) and 800 °C (CS800) in two different magnifications are shown in Fig. 2. It should be mentioned that by using the temperatures before 650 °C, any product was not obtained. Moreover, CS700 image was not shown because it was similar to CS650. According to this figure, all products have spherical shapes, CS750 shows highly uniform spheres with the smallest sizes, while the sizes of spheres in CS650 and CS 800 are larger and their shapes are not as uniforms as those of CS 750, especially for CS800, which deformation and destruction of the spheres could be observed in high values. As shown in the TGA results, this type of material is not so stable at 800 °C and higher temperatures and this deformation confirms their instability at this temperature. Therefore, 750 °C was the optimized growth temperature and CS750 was the selected product for the next analyses and experiments.

To obtain more evidence about the structure of the product, TEM analysis was run for CS750 and the produced images are depicted in Fig. 3. The TEM images confirm the size and morphology of the product. The diameter of spheres was in the range of 500 nm to 1 μm, according to what is seen in the FESEM images. Moreover, the image of spheres is not so dark (which is expected for the dense carbon materials), which propose that they are not totally filled. Therefore, they could be considered as hollowed carbon spheres. To provide some details about the pore structure of the product, the nitrogen adsorption–desorption experiment (using BET theory) was run for CS750 and the obtained diagrams are depicted in Fig. 4. The employed diagram shows type III isotherm with small porosity. The obtained t plot was also confirmed it by showing type I diagrams, related to the non-porous materials. Interestingly, the obtained density was 5.08 mg/cm^3, which shows a very small density of the product. This small density confirms the hollowed structure of the produced spheres, and maybe these materials could be considered as carbon aerogel (Tamon and Olabi 2014).

In the next part, Raman spectroscopy was used to investigate the bonding properties of the carbon networks. Commonly, carbon materials have two characteristics bands, named as G band and D band. The G band indicates the structure of sp^2 hybridized graphitic network and D band is related to the impurities and defects in this network. Both G and D bands were observed in the Raman spectrum of CS750 (Fig. 5), which indicates the presence of a graphite-like structure network with some defects. The G band on 1566 cm^{-1} is more intense than the D band on 1359 cm^{-1}, and the I_D/I_G ratio is 0.93. This value shows the high share of the graphitic structure for this product.

The XRD pattern of the product was recorded to show the details of its crystallinity. In Fig. 6, this pattern is depicted, which shows two peaks of graphitic plates 100° and 002° at 44° and 22°. Both peaks are wide that confirm the product has low crystalline nature. The existence of multiple planes with similar characteristics and close 2θ values is another possible suggestion for these wide peaks. The presence of these graphitic plates is in accordance with the G band observed in Raman spectroscopy. Moreover, any message related to the catalyst compositions (bentonite) has not been observed, showing the purity of the product.

To determine the thermal behavior of the product, TGA and DTA analyses were used and the results are shown in Figs. 7 and 8. As shown in the TGA diagram, the product has not any meaningful weight loss before 260 °C and it only showed a 3% weight loss up to 450 °C. (Fluctuations in the diagram are probably due to the instrumental error.) In the range of 450–620 °C, the weight of the product was remained almost unchanged (less than 1% weight loss). The major part of weight loss for the product was observed after 620 °C, which at the end of the applied temperature (890 °C) it loses totally 19% of its weight (14% at this step). It seems that this product is completely stable in the temperature range up to 620 °C, which makes it a useful candidate for new thermal resistance materials. Most parts of the DTA diagram of the product (Fig. 8) show negative and endothermic signals. These signals imply the degradation and destruction steps. There is only one positive and exothermic DTA signal in 190–360 °C, probably due to the adsorption of the evolved defragmented species or some rearrangements in the product.

To complete the characterization of the product and to define its area of application, the static drop test (as described in the method section) has been employed. The products were so hydrophilic that during this experiment, placing the water drop on the surface of the sample was difficult (Fig. 9). After several repetitions of the experiments and recording the results of successive attempts, the results were extracted. The contact angle of the water drop with the sample surface was measured about 130° (the average of three measurements), which indicates its high hydrophobic (near superhydrophobic) nature.

Fig. 2 The FESEM images of the products at 650 °C (the first row), 750 °C (the second row) and 800 °C (the last row)
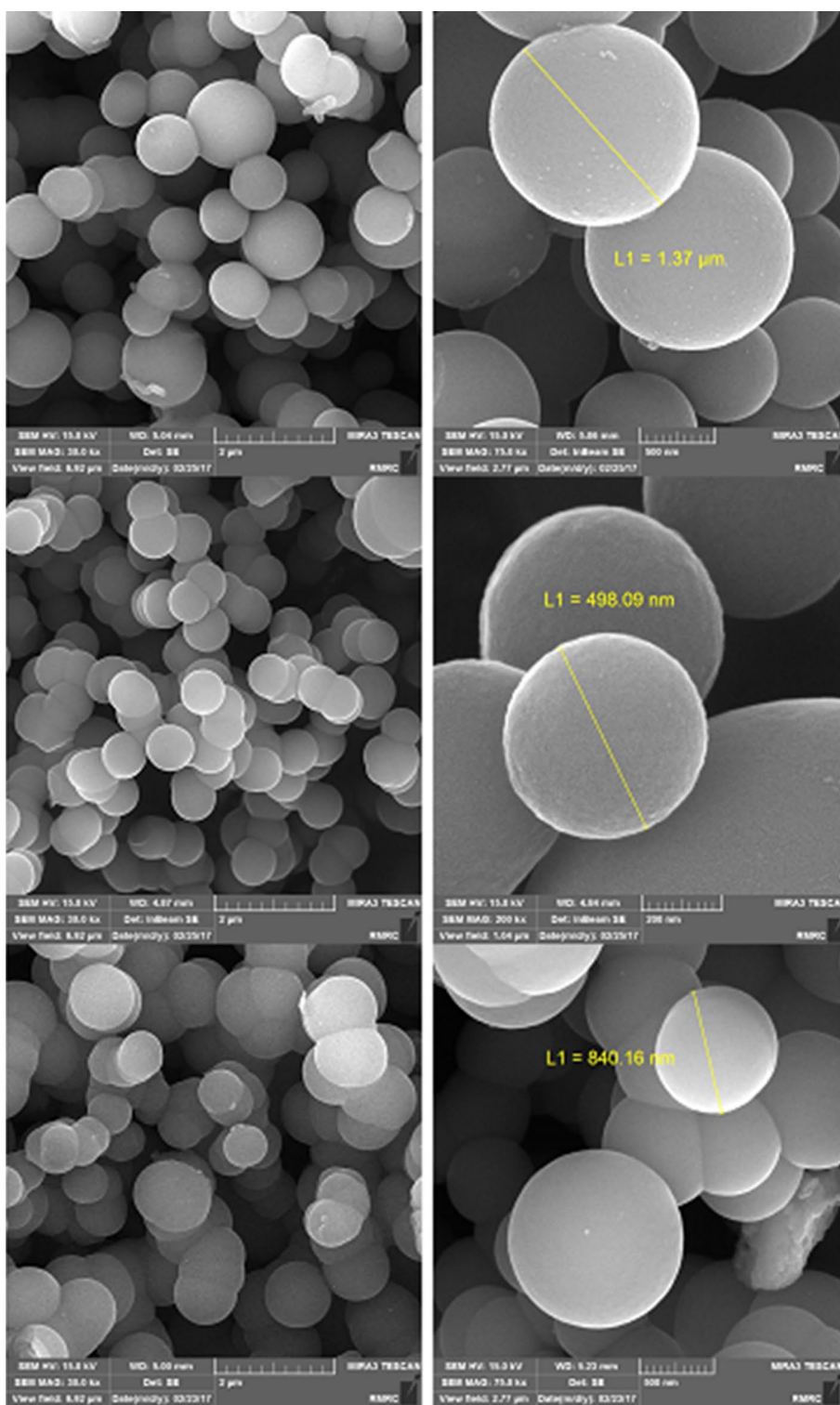
Due to the high hydrophobic nature of the product, it was proposed to consider it for the removal or separation of oil from water. This application has been performed according to the method reported by Pan et al. (Zhu et al. 2010), as described in the method section. According to the reported methodologies, the oil absorption capacity of the adsorbent is determined by weighing the adsorbent before and after the adsorption process, as described in the experimental section.

Fig. 3 TEM images of the selected product, CS750
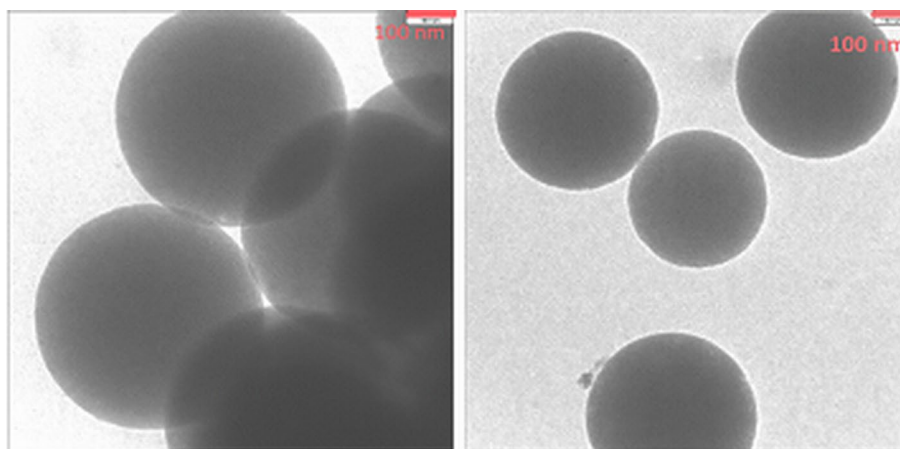
Fig. 4 The adsorption–desorption diagram (left) and t plot (right) of CS750, based on the BET theory
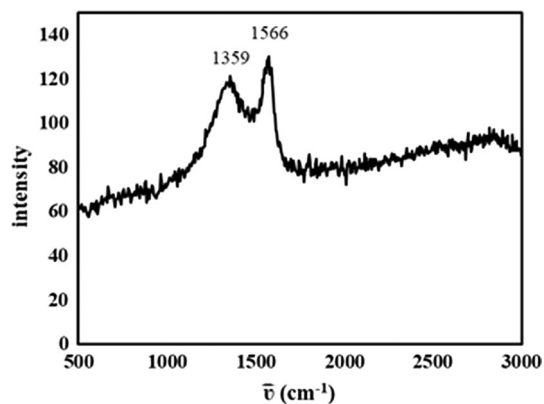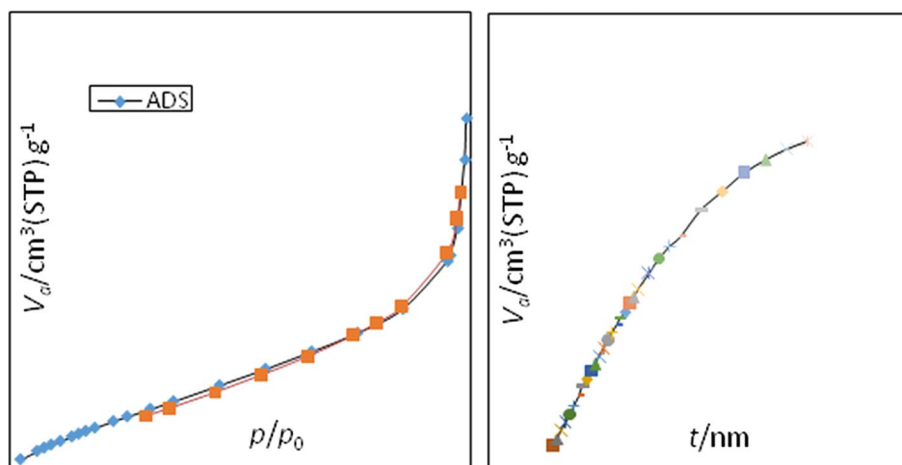

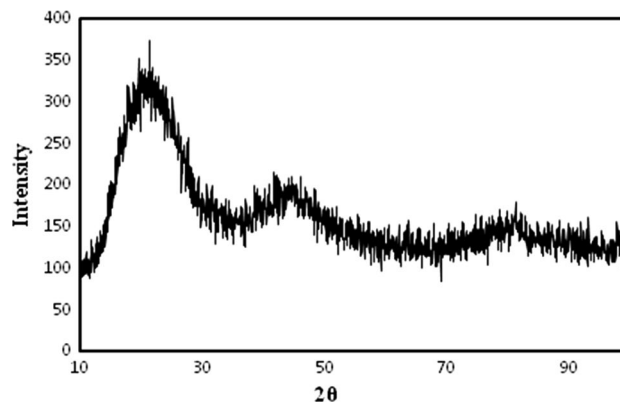**Fig. 5** The Raman spectrum of CS750

Fig. 6 XRD pattern of CS750

In this project, the aqueous emulsion of common oil (Oleic Acid) was selected to examine the adsorption potency of the product. The whole adsorption process was so fast that it was completed in less than 1 s. The adsorbent remains suspended on the surface of the water after absorption and easily removed by simple filtration. In addition, any emulsion, suspension or mixing of the adsorbent with water has not been observed during the process. According to the experiments, the value of q_m (adsorption capacity) for synthesized CS was calculated to 19,000 mg/g and the adsorption (removal)
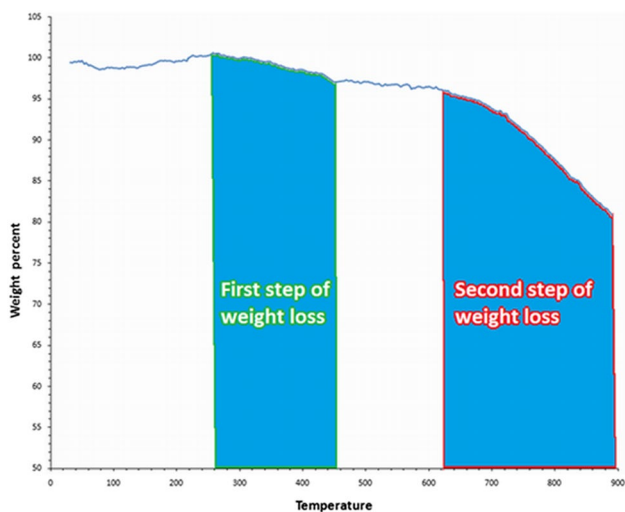
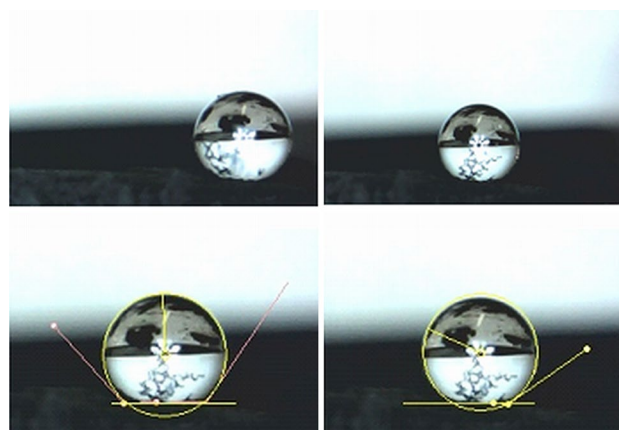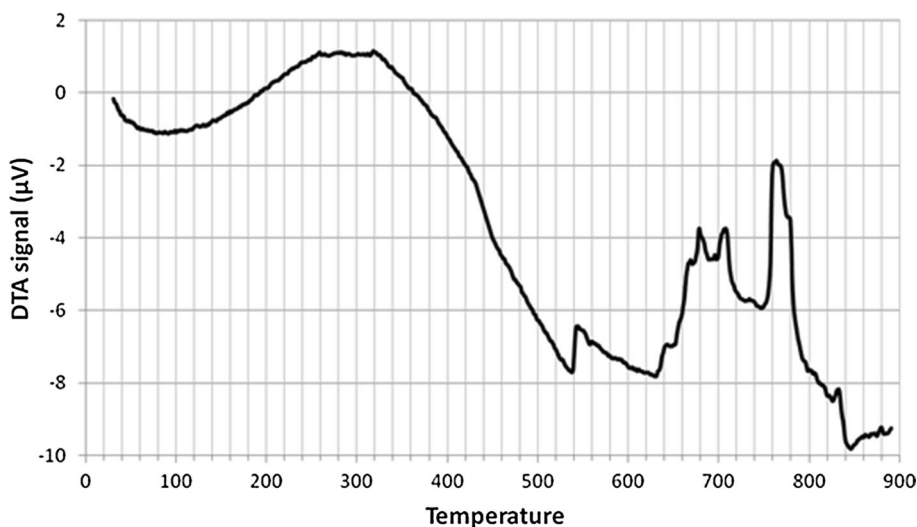**Fig. 7** TGA diagram of the product (CS750)

Fig. 9 The images related to the static contact angle of water drop on the surface of the product. The average value of the contact angle was 130°

efficiency (q_e) was 100%. Therefore, this product could be easily applied for the purification of oily water.

It was tried to examine the kinetics of adsorption. However, because of the ultrafast adsorption process, the whole of this process was completed in less than one second. Therefore, one second was determined as the equilibrium time and it was not possible to study the kinetic models.

Conclusion

An easy procedure for the production of highly hydrophobic and ultrahigh carbon spheres using bentonite as a cheap and available catalyst has been reported. The products were obtained at different temperatures (650–800 °C), but the most uniform spheres were obtained at 750 °C. The diameters of the products were between 500 nm and 1 μm, determined by TEM and FESEM Images. Moreover, TEM images proposed the hollowed shapes for prepared spheres and its calculated density (5.08 mg/cm^3) confirmed this suggestion and proposed that this material could be considered as ultralight material or aerogel. Raman and XRD analyses have confirmed the existence of graphite hexagonal networks of the product. The high hydrophobic nature of the product (with static contact angle = 130°) makes it a potential candidate for oil absorption from the water. Finally, its fast and high oil adsorption potencies were confirmed via the common experiment.

Fig. 8 DTA diagram for CS750. Endothermic processes were shown with negative signals

References

Deshmukh AA, Mhlanga SD, Coville NJ (2010) Carbon spheres. Mater Sci Eng R Rep 70:1–28

Dubey SP, Dwivedi AD, Kim I-C, Sillanpaa M, Kwon Y-N, Lee C (2014) Synthesis of graphene–carbon sphere hybrid aerogel with silver nanoparticles and its catalytic and adsorption applications. Chem Eng J 244:160–167

Evans M, Halliop E, Macdonald J (1999) The production of chemically-activated carbon. Carbon 37:269–274

Falcao EH, Wudl F (2007) Carbon allotropes: beyond graphite and diamond. J Chem Technol Biotechnol Int Res Process Environ Clean Technol 82:524–531

Frolich PK (1936) Carbon black manufacture. Google Patents

Han W, Zhao Y, Dong F, Zhang G, Lu G, Tang Z (2017) Effect of the well-designed functional groups and defects of porous carbon spheres on the catalytic oxidation performance. Microporous Mesoporous Mater 250:35–42

Hassani F, Tavakol H (2018) Synthesis of sulfur-doped carbon nanotubes from sulfur powder using chemical vapor deposition. Fuller Nanotub Carbon Nanostruct 26:479–486

Hoffmann R, Kabanov AA, Golov AA, Proserpio DM (2016) Homo citans and carbon allotropes: for an ethics of citation. Angew Chem Int Ed 55:10962–10976

Jiang J, Gao Q, Zheng Z, Xia K, Hu J (2010) Enhanced room temperature hydrogen storage capacity of hollow nitrogen-containing carbon spheres. Int J Hydrogen Energy 35:210–216

Jin YZ, Gao C, Hsu WK, Zhu Y, Huczko A, Bystrzejewski M, Roe M, Lee CY, Acquah S, Kroto H (2005) Large-scale synthesis and characterization of carbon spheres prepared by direct pyrolysis of hydrocarbons. Carbon 43:1944–1953

Jun Z, Jia-Jia C, Cheng-Long Z, Hang Q, Ming-Sen Z, Quan-Feng D (2014) The synthesis of a core–shell MnO 2/3D-ordered hollow carbon sphere composite and its superior electrochemical capability for lithium ion batteries. J Mater Chem A 2:6343–6347

Kumar M, Ando Y (2010) Chemical vapor deposition of carbon nanotubes: a review on growth mechanism and mass production. J Nanosci Nanotechnol 10:3739–3758

Lee J, Kim J, Hyeon T (2006) Recent progress in the synthesis of porous carbon materials. Adv Mater 18:2073–2094

Li W, Chen D, Li Z, Shi Y, Wan Y, Huang J, Yang J, Zhao D, Jiang Z (2007) Nitrogen enriched mesoporous carbon spheres obtained by a facile method and its application for electrochemical capacitor. Electrochem Commun 9:569–573

Li Q, Jiang R, Dou Y, Wu Z, Huang T, Feng D, Yang J, Yu A, Zhao D (2011) Synthesis of mesoporous carbon spheres with a hierarchical pore structure for the electrochemical double-layer capacitor. Carbon 49:1248–1257

Liang C, Li Z, Dai S (2008) Mesoporous carbon materials: synthesis and modification. Angew Chem Int Ed 47:3696–3717

Liang X, Wen Z, Liu Y, Zhang H, Huang L, Jin J (2011) Highly dispersed sulfur in ordered mesoporous carbon sphere as a composite cathode for rechargeable polymer Li/S battery. J Power Sources 196:3655–3658

Lu C, Chung Y-L, Chang K-F (2006) Adsorption thermodynamic and kinetic studies of trihalomethanes on multiwalled carbon nanotubes. J Hazard Mater 138:304–310

Manawi YM, Samara A, Al-Ansari T, Atieh MA (2018) A review of carbon nanomaterials' synthesis via the chemical vapor deposition (CVD) method. Materials 11:822

Manoukian M, Tavakol H, Fashandi H (2018) Synthesis of highly uniform sulfur-doped carbon sphere using CVD method and its application for cationic dye removal in comparison with undoped product. J Environ Chem Eng 6(6):6904–6915

Miao J-Y, Hwang DW, Narasimhulu KV, Lin P-I, Chen Y-T, Lin S-H, Hwang L-P (2004) Synthesis and properties of carbon nanospheres grown by CVD using Kaolin supported transition metal catalysts. Carbon 42:813–822

Mohammadi F, Tavakol H (2018) Synthesis of phosphorus doped carbon nanotubes using chemical vapor deposition. Fuller Nanotub Carbon Nanostruct 26:218–225

Qian H-S, Han F-M, Zhang B, Guo Y-C, Yue J, Peng B-X (2004) Non-catalytic CVD preparation of carbon spheres with a specific size. Carbon 42:761–766

Shafeeyan MS, Daud WMAW, Houshmand A, Shamiri A (2010) A review on surface modification of activated carbon for carbon dioxide adsorption. J Anal Appl Pyrol 89:143–151

Sichel EK, Gittleman JI, Sheng P (1978) Transport properties of the composite material carbon-poly (vinyl chloride). Phys Rev B 18:5712

Slyh JA, Milton J, Doying EG (1950) Production of activated carbon. Google Patents

Sung JH, Back SK, Lee ES, Jang HN, Seo YC, Kang YS, Lee MH (2019) Application of powdered activated carbon coating to fabrics in a hybrid filter to enhance mercury removal. J Environ Sci 80:58–65

Tamon H, Olabi A (2014) Carbon aerogels. Elsevier, Amsterdam

Tavakol H, Keshavarzipour F (2016) A sulfur doped carbon nanotube as a potential catalyst for the oxygen reduction reaction. RSC Adv 6:63084–63090

Wen Z, Wang Q, Zhang Q, Li J (2007) Hollow carbon spheres with wide size distribution as anode catalyst support for direct methanol fuel cells. Electrochem Commun 9:1867–1872

Wickramaratne NP, Jaroniec M (2013) Activated carbon spheres for CO_2 adsorption. ACS Appl Mater Interfaces 5:1849–1855

Wu J, Hu F, Hu X, Wei Z, Shen PK (2008) Improved kinetics of methanol oxidation on Pt/hollow carbon sphere catalysts. Electrochim Acta 53:8341–8345

Wu G, Cheng Y, Ren Y, Wang Y, Wang Z, Wu H (2015) Synthesis and characterization of γ-Fe_2O_3@ C nanorod-carbon sphere composite and its application as microwave absorbing material. J Alloy Compd 652:346–350

Yang Y, Chiang K, Burke N (2011) Porous carbon-supported catalysts for energy and environmental applications: a short review. Catal Today 178:197–205

Zheng F, Xia B (2017) Application of activated carbon fiber in functional clothing. Chem Eng Trans 59:199–204

Zhu Q, Tao F, Pan Q (2010) Fast and selective removal of oils from water surface via highly hydrophobic core–shell Fe_2O_3@ C nanoparticles under magnetic field. ACS Appl Mater Interfaces 2:3141–3146

Affiliations

P. Bakhshi[1] · H. Tavakol[1]

✉ H. Tavakol
h_tavakol@cc.iut.ac.ir

[1] Department of Chemistry, Isfahan University of Technology, Isfahan 84156-83111, Iran